Chemical synthesis of the ATAD2 bromodomain

Gardner S. Creech[a], Chelsea Paresi[b,c], Yue-Ming Li[b,c], and Samuel J. Danishefsky[a,d,1]

[a]Bioorganic Chemistry Laboratory, Molecular Pharmacology and Chemistry Program, Memorial Sloan-Kettering Cancer Center, New York, NY 10065; [b]Department of Pharmacology, Weill Graduate School of Medical Sciences of Cornell University, New York, NY 10021; [c]Molecular Pharmacology and Chemistry Program, Memorial Sloan-Kettering Cancer Center, New York, NY 10065; and [d]Department of Chemistry, Columbia University, New York, NY 10027

Contributed by Samuel J. Danishefsky, January 10, 2014 (sent for review October 19, 2013)

Due to the emerging importance of the bromodomain binding region in the study of epigenetic effectors and the vast implications for a wide variety of human disease, the bromodomain region of human ATPase family AAA+ (ATPases associated with diverse cellular activities) domain-containing protein 2 (ATAD2) was targeted for chemical synthesis. The ATAD2 bromodomain (130 aa) was divided into five strategic fragments to be assembled using native chemical ligation with a focus on maximal convergency and efficiency. The fragments were assembled with one cysteine and three thioleucine ligations, unveiling the native alanine and leucine amino acids at the ligation points following metal-free dethiylation. Synthetic highlights of the study are a photolabile dimethoxynitrobenzyl-protected glutamic acid side chain used to impede hydrolysis of the C-terminal Glu-thioester, a thiazolidine-protected thioleucine, and an efficient assembly of three fragments in a single reaction vessel with dual-mode kinetic-standard chemical ligation. With a focus on material throughput and convergency, the five peptide fragments were assembled into the native ATAD2 bromodomain region with a total of three HPLC events in 8% overall yield from the fragments.

solid-phase peptide synthesis | desulfurization | peptide retrosynthesis

Concurrent with increased understanding of epigenetic regulation of the proteome is the discovery of new modalities in which aberrant epigenetic states can lead to disease. One such example, the bromodomain–protein binding motif, is a family of 47 human epigenetic reader proteins that have been shown to bind to the *N*-acetylated lysines of histones. The bromodomain was named for the brahma gene in *Drosophila*, mutations of which led to the discovery of the related peptide domain in humans (1). As such, they have been increasingly implicated in disease states as far reaching as cancer, HIV, and diabetes (2–5). Given their effect on functions ranging from chromatin remodeling and transcriptional regulation, it is not surprising that a great deal of effort has been focused on therapeutic intervention at the level of bromodomain-containing proteins. Much of this work has been focused on the bromodomain and extraterminal family of proteins and has resulted in advancing several chemical entities for clinical consideration (6–11). [For a selection of relevant clinical trials: Constellation Pharmaceuticals, CPI-0610; OncoEthix, OTX015 (NCT01713582); Resverlogix Corp., RVX-208 (NCT00768274, NCT01067820, NCT01423188, NCT01058018, NCT01728467, NCT01863225); GlaxoSmithKline, GSK525762 (NCT01943851, NCT01587703).]

An additional bromodomain-containing protein that has been identified as a potential target for therapeutic intervention is ATPase family AAA+ (ATPases associated with diverse cellular activities) domain-containing protein 2 (ATAD2; also referred to as ANCCA, AAA+ nuclear coactivator cancer–associated), which is a human protein composed of two ATPase domains and a bromodomain motif (Fig. 1; refs. 12, 13). In numerous cell lines, ATAD2 has been shown to be the driver of c-Myc–induced cell growth. Although c-Myc is one of the best known oncogenes, at present there has been no reported clinical progress based on interventions at the level of c-Myc (14–16). ATAD2 is also implicated in estrogen-induced tumor growth in breast and ovarian cancer cells and in androgen-induced growth of prostate cancer cells by acting as a target for the E2F family of transcription factors (17–21). Furthermore, ATAD2 has been shown to induce transcription of c-Myc, as well as the estrogen and androgen receptors. Indeed, ATAD2 has been identified as highly up-regulated in a wide variety of tumor cell lines. For instance, it has been found to be highly up-regulated in a genomic analysis of lung cancers, ovarian cancers, and inflammatory breast cancer (the most aggressive form of breast cancer; refs. 14–16, 22–25). Moreover, recent studies have served to correlate ATAD2 expression with poor prognosis in a variety of tumor types (14, 15, 23, 24, 26). Finally, RNA interference of ATAD2 has shown a variety of promising outcomes, including inhibition of tumor growth and induction of apoptosis (14, 16, 17, 19, 23, 24).

Chemical synthesis of the bromodomain motif could facilitate numerous avenues for further study, including enabling access to family members that have, thus far, not been accessible by recombinant technology (27). Accordingly, current studies of the bromodomain family have focused predominantly on regions removed from the environment of the full protein. Access to high-purity synthetic material would assist establishing in detail that the truncated bromodomain regions serve as a reliable model for binding of the full-length bromodomain-containing proteins. In regards to ATAD2, contrasting histone binding sites have been identified in full-length versus bromodomain motif proteins. Immunoprecipitation experiments of cell lysates with ectopic expression of full-length ATAD2 demonstrated that it binds to histone H3 acetylated at lysine 14 (H3K14Ac) (14, 19). In contrast, in a SPOT array of truncated bromodomain motifs with histone mimics, the preferential site of binding was identified as H2AK36Ac, with H2BK85Ac binding more weakly (27). Chemical synthesis would also provide access to D-proteins, which are of potential use in mirror-image phage display for the discovery of short D-peptide inhibitors (28, 29). Another application of synthetic D-proteins could also involve their facilitation

Significance

The bromodomain–histone binding motif has been shown to read epigenetic marks on chromatin, and proteins with a bromodomain can have powerful effects on gene expression and transcriptional regulation. ATAD2 is one such protein and has been linked to a wide variety of cancers with expression of ATAD2 correlating strongly with a poor tumor prognosis. We have developed an efficient chemical synthesis of the ATAD2 bromodomain region using modern ligation methods to assemble peptide fragments. Lessons learned in this synthetic exploration include a number of potentially general solutions that expand the disconnection vocabulary, as well as lessons that maximize the convergency and throughput in the chemical synthesis of proteins.

Author contributions: G.S.C., C.P., Y.-M.L., and S.J.D. designed research; G.S.C. and C.P. performed research; Y.-M.L. contributed new reagents/analytic tools; G.S.C., C.P., Y.-M.L., and S.J.D. analyzed data; and G.S.C. and S.J.D. wrote the paper.

The authors declare no conflict of interest.

[1]To whom correspondence should be addressed. E-mail: s-danishefsky@ski.mskcc.org.

This article contains supporting information online at www.pnas.org/lookup/suppl/doi:10.1073/pnas.1400556111/-/DCSupplemental.

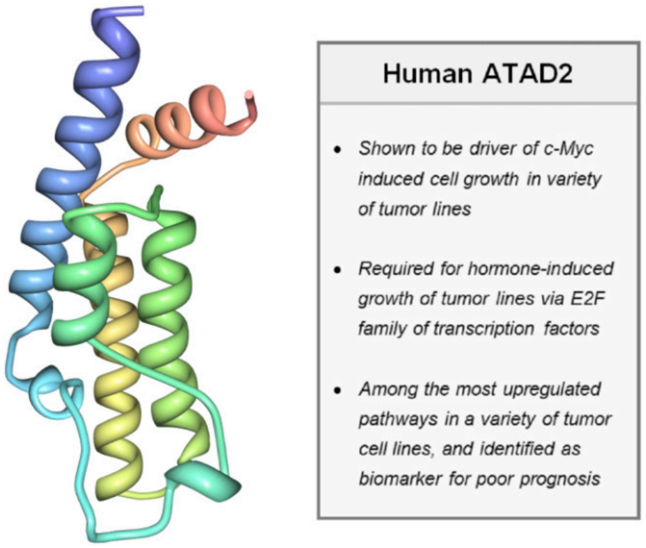

Fig. 1. Crystal structure of the bromodomain region of ATAD2 (11).

of protein crystallization based on the observation that a racemic mixture of L- and D-proteins has an increased probability of crystallization (30, 31).

Results and Discussion

In devising our retrosynthetic strategy to arrive at the ATAD2 bromodomain (Ser979–Arg1108, **1**), high priority was assigned to optimal convergency. Another important consideration was the adaptability of the general strategy for achieving diverse analogs, such as histidine-tagged or fluorescently tagged analogs or bromodomain regions fused to a cell-penetrating peptide sequence. It was envisioned that the 130-mer peptide target would be "disconnected" into four or five fragments of reasonable size (Fig. 2). Enabling the connecting of these fragments was the pioneering work of Kent and coworkers, which resulted in the discovery and development of native chemical ligation (NCL) (32). Native chemical ligation has developed into a powerful means for accessing proteins of reasonable size through synthetic means. The possibility of extending the reach of NCL to include alanine ligation was demonstrated by Dawson and coworker via metal-induced dethiylation of the cysteine at the N terminus of the ligation site (33). Subsequently, metal-free dethiylation (MFD) (34) resulted in a major expansion of NCL by enabling disconnection strategies of alanine, valine, leucine, threonine, and proline, among others. In the convergent retrosynthesis as planned in this work, the first disconnection was between the second and third fragment (F2 and F3), so as to avoid the necessity of tandem kinetic ligations (35) in the assembly of the first half. Thus, to take advantage of the Leu22–Ala23 disconnection site for alanine ligation and obviate the construction an Ala22–Ile78 second fragment, the F2–F3 disconnection site we favored was at Tyr65–Leu66. With the final ligation planned to be a thioleucine ligation (the necessity of desulfurization precludes the cysteine ligation at Cys101 or Cys123), disconnections between Asn86–Pro87, Arg94–Leu95, and Glu114–Leu115 were envisioned. The reduction to practice of this line of thinking, resulting in the chemical synthesis of the ATAD2 bromodomain, is described below.

Fragment F1 thioester (Ser1–Leu22, **2**) was synthesized following standard solid-phase peptide synthesis (SPPS) protocols. The protected peptide was cleaved, followed by C-terminal attachment of the leucine thiophenyl thioester and global deprotection; thus, peptide **2**, purified by reverse-phase (RP)-HPLC, was in hand (33% yield). Under the same SPPS protocols, fragment F2 (Cys23–Tyr65, **3**) was isolated in only 9% yield due to a high level of aspartimide formation. Application of the Asp (OMpe) derivative (Fmoc-(O-3-methyl-pent-3-yl)aspartic acid, commercially available) (36) and a strategically placed pseudoproline dipeptide at Ile57–Ser58 increased the isolated yield following RP-HPLC to 35% (37, 38). Following subjection of peptide fragments **2** and **3** to kinetic ligation buffer [6 M guanidinium hydrochloride (Gnd), 200 mM phosphate buffer, 20 mM *tris*(2-carboxyethyl)phosphine (TCEP), pH 7.2] (34), formation of the ligated product **4** was confirmed by liquid chromatography–mass spectrometry (LC-MS) (Fig. 3). Further reaction of **4** was observed with fragment **2**, and an adduct **5** with two equivalents of **2** per fragment **3** was also obtained (compound **5**) (Fig. 3*A*). Subsequent addition of exogenous alkyl thiol to the reaction mixture served to cleave the additional transthioester and yield the desired **4** peptide upon RP-HPLC (55%) (Fig. 3*B*).

The synthesis of the second target intermediate Leu66–Arg130 was pursued next (Fig. 4). To engage the third and fourth fragments in a kinetic leucine ligation (39), it was necessary to protect the N terminus of F3 as a thioleucine thiazolidine. In the event, fragment **6** and fragment **7** with an N-terminal thioproline failed to undergo kinetic ligation to form **8** with the predominant products arising from hydrolysis of the thioester, **9** (40), and macrocyclization of fragment **7** resulting in **10**. It is possible that both thioester hydrolysis and macrocyclization of fragment **7**

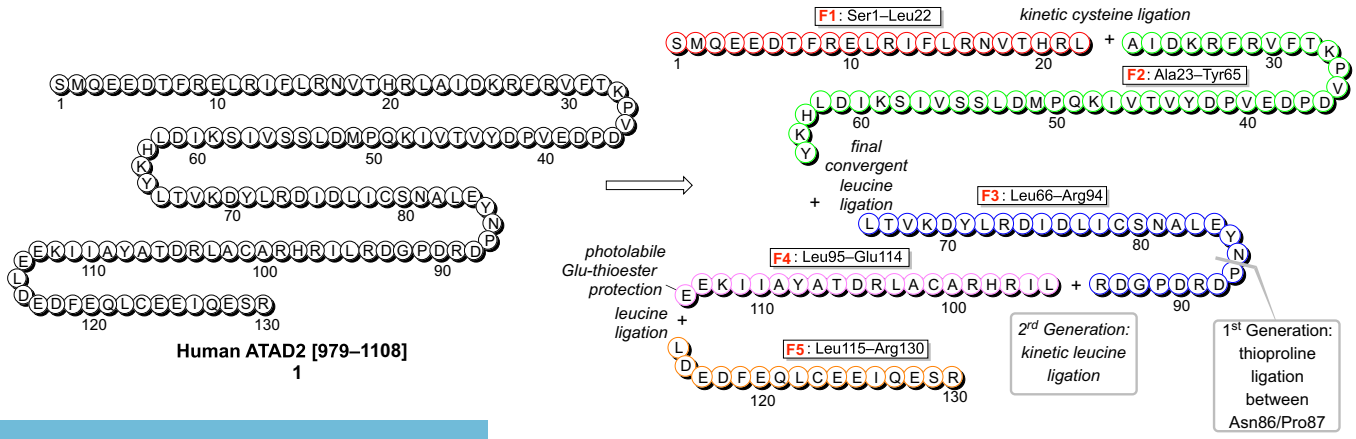

Fig. 2. Retrosynthesis of the bromodomain region of ATAD2 [979–1108].

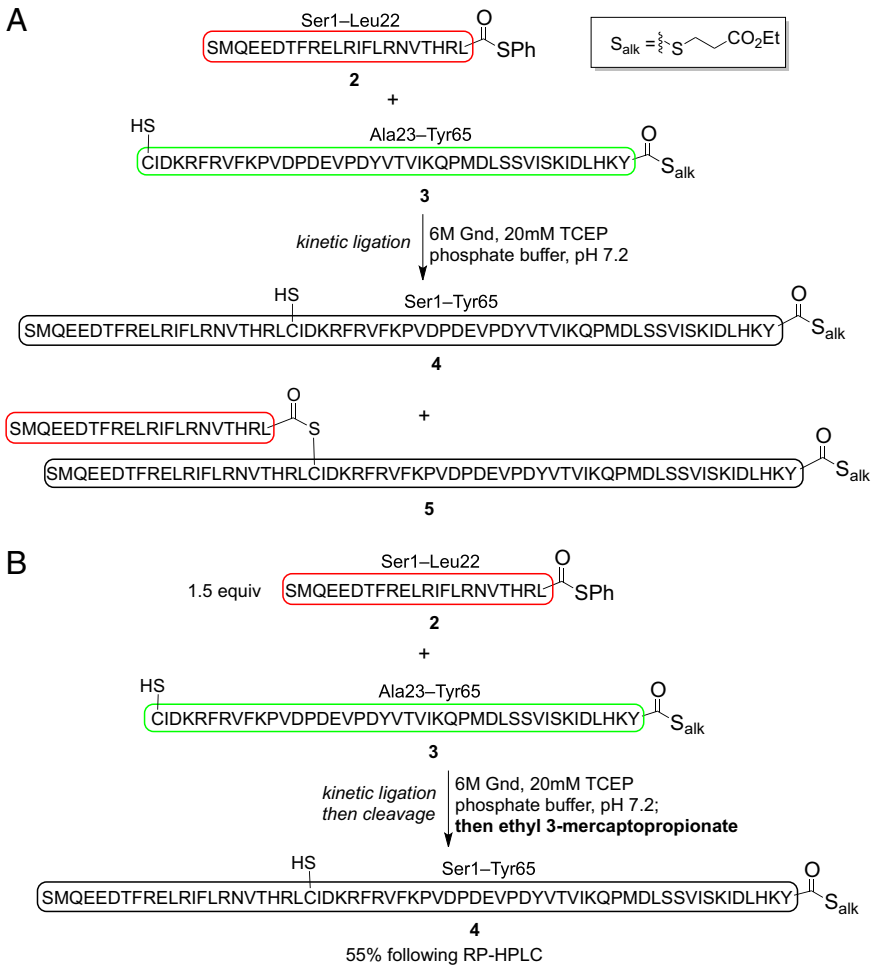

Fig. 3. Kinetic ligation of fragments F1 and F2 for the synthesis of Ser1–Tyr65. (*A*) Under standard conditions, the desired product was observed to undergo further transthioesterification to yield 5. (*B*) Side product 5 could be cleaved to the desired fragment 4 with the addition of exogenous alkyl thiol upon completion.

result from a reactive intermediate glutamic anhydride. In this case, the Pro-Glu peptide bond could be an α- or γ-linkage; no effort was made to distinguish between the two.

We then probed the ligation between Arg94–Leu95. In general, thioleucine ligation has been observed to be more reliable than the thioproline ligation. To circumvent the problematic

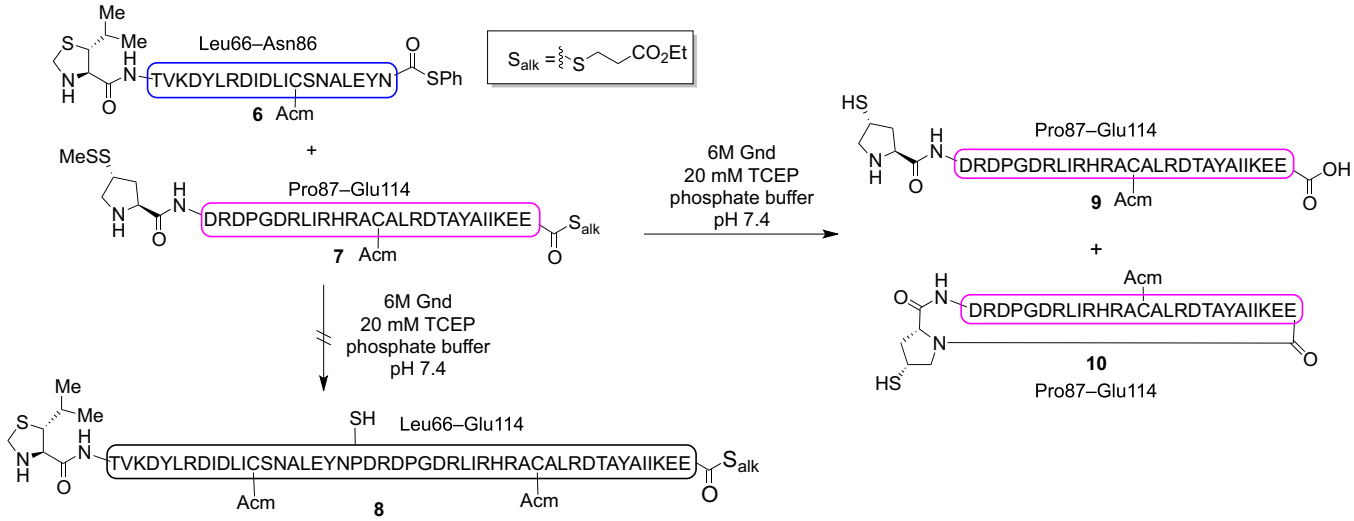

Fig. 4. First generation ligation of fragments F3 and F4 via thioproline ligation, with products predominantly resulting from thioester hydrolysis and macrocyclization of fragment **7**. Acm = acetamidomethyl.

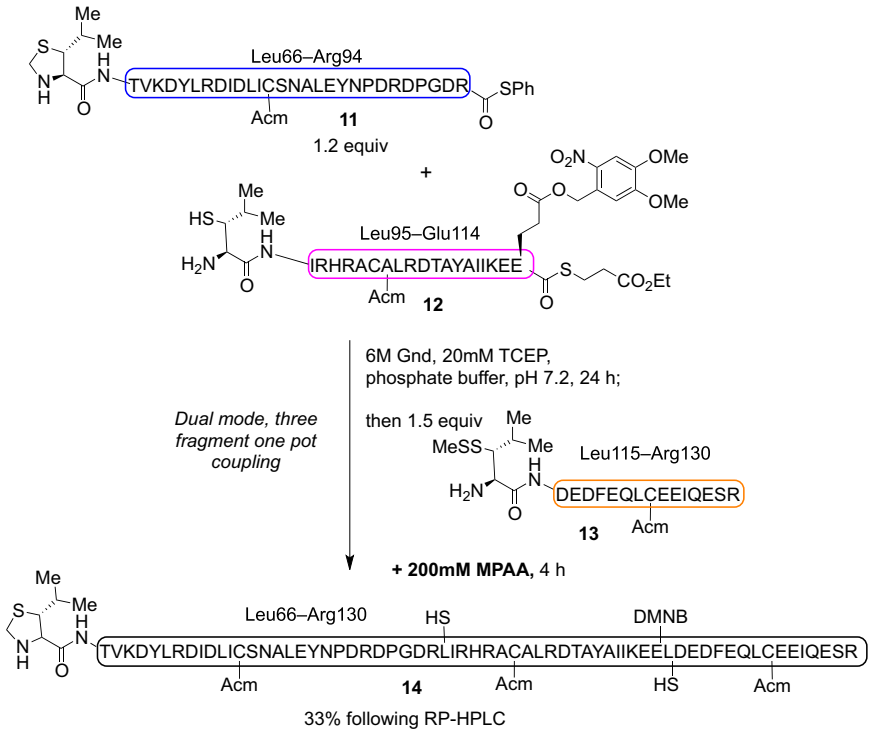

Fig. 5. Three-fragment, one-pot dual ligation strategy for the assembly of Leu66–Arg130 fragment from fragments F3, F4, and F5.

thioester hydrolysis, the glutamic acid side chain was protected as a dimethoxynitrobenzyl ester (DMNB), which we imagined could undergo photolytic cleavage without the requirement of an additional RP-HPLC purification (Fig. 5; ref. 41). With the previously stated goal of maximizing convergency and efficiency of the synthetic route, it was hypothesized that the Leu66–Arg130 fragment could be formed in a one-pot, dual-ligation strategy. This hope hinged on the observation that the *N* and C termini of the targeted Leu66–Arg130 fragment **14** were both constitutionally disarmed, lacking the opportunity for cross-reactivity that would traditionally prevent such a strategy. In the event, a slight excess of fragment **11** was joined with **12** in a kinetic ligation buffer, added to fragment **13** predissolved in 4-mercaptophenylacetic acid (MPAA) NCL buffer to switch the reaction mode from kinetic to standard NCL. It is worth noting that the additional trans-thioesterification to yield **5** in the kinetic cysteine ligation (see above) was not observed in the kinetic thioleucine ligation between **11** and **12**, perhaps because of the increased steric bulk of the thioleucine. Following RP-HPLC purification, Leu66–Arg130 **14** was isolated in 33% yield.

Before joining the penultimate fragments **4** and **14** of the ATAD2 bromodomain to realize the convergent synthesis, the

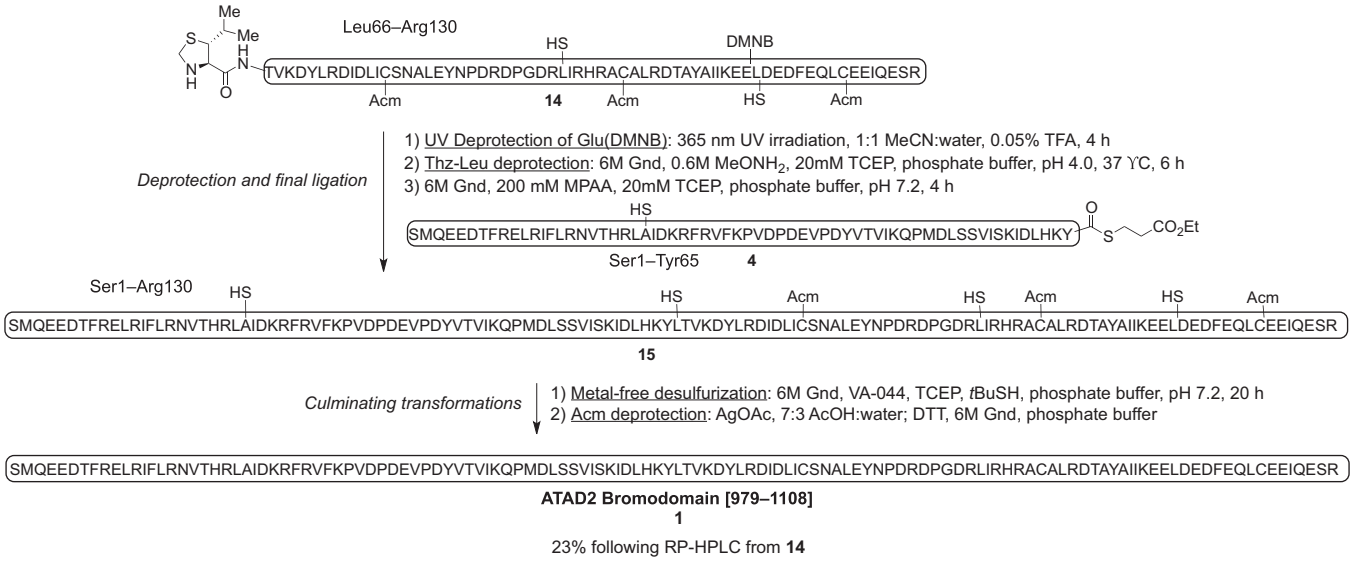

Fig. 6. Convergent assembly of peptides Ser1–Tyr65 and Leu66–Arg130 for the completion of the ATAD2 bromodomain. DTT = DTT, VA-044 = 2,2′-azobis[2-(2-imidazolin-2-yl)propane]dihydrochloride.

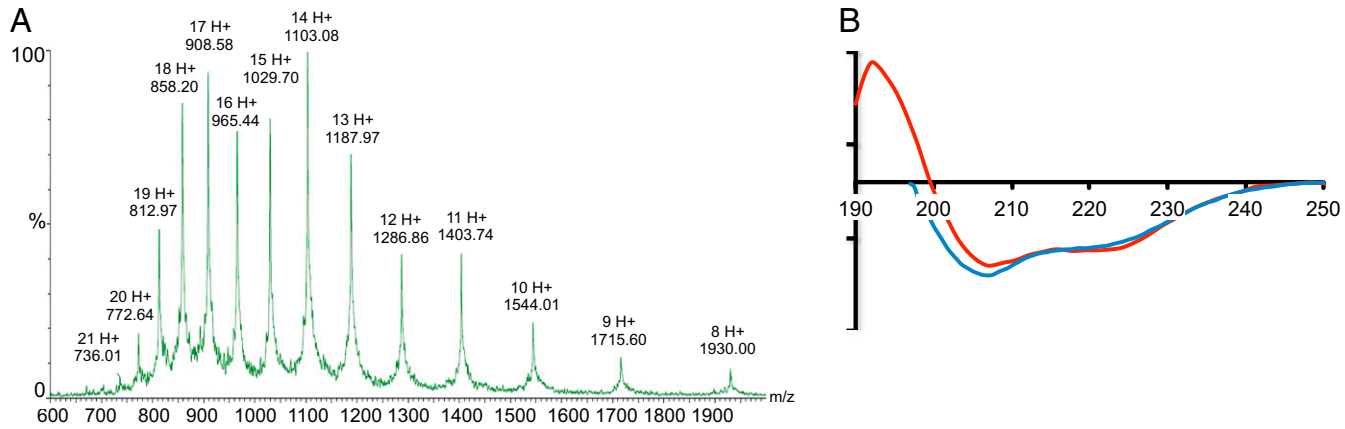

Fig. 7. Spectral analysis of fully synthetic ATAD2 bromodomain **1**. (*A*) LC-MS of **1** following purification. Calcd. for $C_{679}H_{1083}N_{189}O_{211}S_5$ 15430.55 Da (average isotopes); observed 15430.54, average of molecular ion peaks as shown. (*B*) CD spectra of the chemically synthesized ATAD2 bromodomain in pH 7.0 phosphate buffer (red) and PBS buffer with 0.05% Tween-20 (blue).

Leu66–Arg130 fragment **14** required deprotection of both the DMNB group and the thiazolidine (Fig. 6). Peptide functionalities and side chains are known to be tolerant of the near-UV 365-nm irradiation that is required for deprotection (42, 43). Photolysis of the Glu(DMNB) residue occurred rapidly and cleanly in acetonitrile/water when subjected to 365-nm longwave UV irradiation. It is worth noting that no special equipment was necessary to induce photolysis, and a standard longwave TLC lamp was used. Upon completion of the photolysis, the reaction mixture was directly lyophilized without further workup or handling. Subsequently, the *N*-terminal thioleucine was unveiled smoothly as well, and subsequent ligation to fragment **4** resulted in antepenultimate full-length intermediate **15**. MFD of the ligation points revealed Ala23, Leu66, Leu95, and Leu115, and Acm-deprotection led to the native ATAD2 bromodomain binding region [979–1108], **1**.

The ATAD2 bromodomain is composed of a primarily α-helical secondary structure with the helices arranged in a left-handed bundle. In addition, the folded native protein lacks intramolecular disulfide bonds to stabilize the ternary structure, so it was not necessary to subject the synthetic peptide to the commonly applied redox folding buffers. Acquisition of the circular dichroism (CD) spectrum of the synthetic bromodomain that was allowed to equilibrate either in pH 7 phosphate buffer or PBS buffer containing Tween detergent resulted in a spectrum with double minima at 208 and 222 nm that is characteristic of primarily α-helical structures (Fig. 7). The CD spectrum provided evidence that the synthetic peptide was able to spontaneously fold into the proposed native structure.

In conclusion, we have achieved a robust synthesis of the ATAD2 bromodomain-binding region. The governing logic involved disconnection of the 130-mer peptide into five fragments, which were assembled in a highly convergent manner with only three total RP-HPLC events to maximize material throughput. The chemical synthesis features several points of innovation, including the first application of thiazolidine-protected thioleucine and its deprotection, the rapid assembly of three fragments in one reaction vessel, and a photolabile DMNB-protected C-terminal glutamic acid thioester to circumvent thioester hydrolysis during the ligation event. It seems likely that this line of thinking and the innovations resulting from its synthesis can find application to other target polypeptides. Efforts are ongoing to quantify the binding of the synthetic ATAD2 bromodomain with histone mimics using a variety of assay techniques to rigorously establish the ATAD2 binding interaction and the viability of using bromodomain fragments to reconstitute the binding interaction of the full-length ATAD2.

Materials and Methods

All commercially available reagents were used without further purification (see *SI Appendix* for vendor list). Ligations were performed under a degassed, argon atmosphere; all other reactions were performed under an atmosphere of nitrogen. NMR spectra (^1H and ^{13}C) were recorded on a Bruker Advance II 600 MHz or Bruker Advance DRX-500 MHz. LC-MS analyses and mass spectrometry data were collected with a Waters Micromass ZQ mass spectrometer. Automated peptide synthesis was performed on an Applied Biosystems Pioneer continuous flow peptide synthesizer under standard Fmoc protocol, NovaSyn TGT resins, 1-[bis(dimethylamino)methylene]-1H-1,2,3-triazolo[4,5-b]pyridinium 3-oxid hexafluorophosphate (HATU) activation, and 96:2:2 dimethylformamide/piperidine/1,8-diazabicyclo[5.4.0]undec-7-ene (DBU) as deblock solution. Reaction progress was monitored on a Waters Acquity UPLC equipped with photodiode detector and single quadrupole mass detector. Preparative separations were performed using a Waters HPLC system using Agilent Dynamax RP-250 × 21.4mm C8 or C4 columns. Buffers for ligation, deprotection, and dethiylation were prepared to the concentrations described, adjusted to the appropriate pH with 5M sodium hydroxide or 2M hydrogen chloride, and degassed with argon sparge under sonication for 30 min. Whatman Integral Comparison Strip, 6.0–8.1 or 3.8–5.5 ranges were used to measure buffer pH.

ACKNOWLEDGMENTS. We thank Dr. J. Fraser Glickman, Brendan Smith, and Antonio Luz for use of the surface plasmon resonance facilities and training. We thank Dr. Lisa Ambrosini Vadola for assisting in the preparation of this manuscript. We acknowledge the National Institutes of Health for funding for this research (GM102872-34 to S.J.D.), as well as for postdoctoral support (F32 GM101746 to G.S.C.) and predoctoral support (5T32GM073546-07 to C.P.).

1. Tamkun JW, et al. (1992) Brahma: A regulator of Drosophila homeotic genes structurally related to the yeast transcriptional activator SNF2/SWI2. *Cell* 68(3):561–572.
2. Muller S, Filippakopoulos P, Knapp S (2011) Bromodomains as therapeutic targets. *Expert Rev Mol Med* 13:e29.
3. Denis GV, Nikolajczyk BS, Schnitzler GR (2010) An emerging role for bromodomain-containing proteins in chromatin regulation and transcriptional control of adipogenesis. *FEBS Lett* 584(15):3260–3268.
4. Denis GV (2010) Bromodomain coactivators in cancer, obesity, type 2 diabetes, and inflammation. *Discov Med* 10(55):489–499.
5. Barbieri I, Cannizzaro E, Dawson MA (2013) Bromodomains as therapeutic targets in cancer. *Brief Funct Genomics* 12(3):219–230.
6. Filippakopoulos P, et al. (2010) Selective inhibition of BET bromodomains. *Nature* 468(7327):1067–1073.
7. Nicodeme E, et al. (2010) Suppression of inflammation by a synthetic histone mimic. *Nature* 468(7327):1119–1123.
8. Ito T, et al. (2011) Real-time imaging of histone H4K12-specific acetylation determines the modes of action of histone deacetylase and bromodomain inhibitors. *Chem Biol* 18(4):495–507.

9. Chung CW, et al. (2011) Discovery and characterization of small molecule inhibitors of the BET family bromodomains. *J Med Chem* 54(11):3827–3838.
10. Dhalluin C, et al. (1999) Structure and ligand of a histone acetyltransferase bromodomain. *Nature* 399(6735):491–496.
11. Zeng L, et al. (2005) Selective small molecules blocking HIV-1 Tat and coactivator PCAF association. *J Am Chem Soc* 127(8):2376–2377.
12. Boussouar F, Jamshidikia M, Morozumi Y, Rousseaux S, Khochbin S (2013) Malignant genome reprogramming by ATAD2. *Biochim Biophys Acta* 1829(10):1010–1014.
13. Hsia EY, Goodson ML, Zou JX, Privalsky ML, Chen HW (2010) Nuclear receptor coregulators as a new paradigm for therapeutic targeting. *Adv Drug Deliv Rev* 62(13): 1227–1237.
14. Ciró M, et al. (2009) ATAD2 is a novel cofactor for MYC, overexpressed and amplified in aggressive tumors. *Cancer Res* 69(21):8491–8498.
15. Fouret R, et al. (2012) A comparative and integrative approach identifies ATPase family, AAA domain containing 2 as a likely driver of cell proliferation in lung adenocarcinoma. *Clin Cancer Res* 18(20):5606–5616.
16. Raeder MB, et al. (2013) Integrated genomic analysis of the 8q24 amplification in endometrial cancers identifies ATAD2 as essential to MYC-dependent cancers. *PLoS ONE* 8(2):e54873.
17. Zou JX, Revenko AS, Li LB, Gemo AT, Chen HW (2007) ANCCA, an estrogen-regulated AAA+ ATPase coactivator for ERalpha, is required for coregulator occupancy and chromatin modification. *Proc Natl Acad Sci USA* 104(46):18067–18072.
18. Zou JX, et al. (2009) Androgen-induced coactivator ANCCA mediates specific androgen receptor signaling in prostate cancer. *Cancer Res* 69(8):3339–3346.
19. Revenko AS, Kalashnikova EV, Gemo AT, Zou JX, Chen HW (2010) Chromatin loading of E2F-MLL complex by cancer-associated coregulator ANCCA via reading a specific histone mark. *Mol Cell Biol* 30(22):5260–5272.
20. Hsia EY, et al. (2010) Deregulated E2F and the AAA+ coregulator ANCCA drive proto-oncogene ACTR/AIB1 overexpression in breast cancer. *Mol Cancer Res* 8(2):183–193.
21. Altintas DM, et al. (2012) Direct cooperation between androgen receptor and E2F1 reveals a common regulation mechanism for androgen-responsive genes in prostate cells. *Mol Endocrinol* 26(9):1531–1541.
22. Ramakrishna M, et al. (2010) Identification of candidate growth promoting genes in ovarian cancer through integrated copy number and expression analysis. *PLoS ONE* 5(4):e9983.
23. Kalashnikova EV, et al. (2010) ANCCA/ATAD2 overexpression identifies breast cancer patients with poor prognosis, acting to drive proliferation and survival of triple-negative cells through control of B-Myb and EZH2. *Cancer Res* 70(22):9402–9412.
24. Caron C, et al. (2010) Functional characterization of ATAD2 as a new cancer/testis factor and a predictor of poor prognosis in breast and lung cancers. *Oncogene* 29(37): 5171–5181.
25. Fernandez SV, et al. (2013) Inflammatory breast cancer (IBC): Clues for targeted therapies. *Breast Cancer Res Treat* 140(1):23–33.
26. Zhang Y, et al. (2013) ANCCA protein expression is a novel independent poor prognostic marker in surgically resected lung adenocarcinoma. *Ann Surg Oncol* 20(Suppl 3):S577–S582.
27. Filippakopoulos P, et al. (2012) Histone recognition and large-scale structural analysis of the human bromodomain family. *Cell* 149(1):214–231.
28. Schumacher TN, et al. (1996) Identification of D-peptide ligands through mirror-image phage display. *Science* 271(5257):1854–1857.
29. Sun N, Funke SA, Willbold D (2012) Mirror image phage display—Generating stable therapeutically and diagnostically active peptides with biotechnological means. *J Biotechnol* 161(2):121–125.
30. Yeates TO, Kent SB (2012) Racemic protein crystallography. *Annu Rev Biophys* 41:41–61.
31. Dang B, Kubota T, Mandal K, Bezanilla F, Kent SB (2013) Native chemical ligation at Asx-Cys, Glx-Cys: Chemical synthesis and high-resolution X-ray structure of ShK toxin by racemic protein crystallography. *J Am Chem Soc* 135(32):11911–11919.
32. Dawson PE, Muir TW, Clark-Lewis I, Kent SB (1994) Synthesis of proteins by native chemical ligation. *Science* 266(5186):776–779.
33. Yan LZ, Dawson PE (2001) Synthesis of peptides and proteins without cysteine residues by native chemical ligation combined with desulfurization. *J Am Chem Soc* 123(4):526–533.
34. Wan Q, Danishefsky SJ (2007) Free-radical-based, specific desulfurization of cysteine: A powerful advance in the synthesis of polypeptides and glycopolypeptides. *Angew Chem Int Ed Engl* 46(48):9248–9252.
35. Bang D, Pentelute BL, Kent SB (2006) Kinetically controlled ligation for the convergent chemical synthesis of proteins. *Angew Chem Int Ed Engl* 45(24):3985–3988.
36. Karlström A, Undén A (1996) A new protecting group for aspartic acid that minimizes piperidine-catalyzed aspartimide formation in Fmoc solid phase peptide synthesis. *Tetrahedron Lett* 37(24):4243–4246.
37. Ullmann V, et al. (2012) Convergent solid-phase synthesis of N-glycopeptides facilitated by pseudoprolines at consensus-sequence Ser/Thr residues. *Angew Chem Int Ed Engl* 51(46):11566–11570.
38. Wang P, Aussedat B, Vohra Y, Danishefsky SJ (2012) An advance in the chemical synthesis of homogeneous N-linked glycopolypeptides by convergent aspartylation. *Angew Chem Int Ed Engl* 51(46):11571–11575.
39. Tan Z, Shang S, Danishefsky SJ (2010) Insights into the finer issues of native chemical ligation: An approach to cascade ligations. *Angew Chem Int Ed Engl* 49(49):9500–9503.
40. Villain M, Gaertner H, Botti P (2003) Native chemical ligation with aspartic and glutamic acids as C-terminal residues: Scope and limitations. *Eur J Org Chem* (17): 3267–3272.
41. Marriott G (1994) Caged protein conjugates and light-directed generation of protein activity: Preparation, photoactivation, and spectroscopic characterization of caged G-actin conjugates. *Biochemistry* 33(31):9092–9097.
42. Wojcik F, O'Brien AG, Götze S, Seeberger PH, Hartmann L (2013) Synthesis of carbohydrate-functionalised sequence-defined oligo(amidoamine)s by photochemical thiol-ene coupling in a continuous flow reactor. *Chemistry* 19(9):3090–3098.
43. Wright TH, et al. (2013) Direct peptide lipidation through thiol-ene coupling enables rapid synthesis and evaluation of self-adjuvanting vaccine candidates. *Angew Chem Int Ed Engl* 52(40):10616–10619.